Vol. 22: 195–212, 2014
doi: 10.3354/ab00593

AQUATIC BIOLOGY
Aquat Biol

Published November 20

Contribution to the Theme Section 'Environmental forcing of aquatic primary productivity'

Continuous monitoring of *in vivo* chlorophyll *a* fluorescence in *Ulva rigida* (Chlorophyta) submitted to different CO_2, nutrient and temperature regimes

F. L. Figueroa[1,*], R. Conde-Álvarez[1], J. Bonomi Barufi[2], P. S. M. Celis-Plá[1], P. Flores[1], E. J. Malta[3], D. B. Stengel[4], O. Meyerhoff[5], A. Pérez-Ruzafa[6]

[1]Department of Ecology, Faculty of Sciences, University of Malaga, 29071 Malaga, Spain
[2]Departamento de Botânica, Universidade Federal de Santa Catarina, 88040-970 Trindade, Florianópolis, SC, Brazil
[3]Centro IFAPA Agua del Pino, Crtra. El Rompido Punta Umbría, 21459 Cartaya (Huelva), Spain
[4]Botany and Plant Science, School of Natural Sciences, Ryan Institute for Environmental Marine and Energy Research, National University of Ireland Galway, Galway, Ireland
[5]Heinz Walz GmbH, Eichenring 6, 91090 Effeltrich, Germany
[6]Department of Ecology and Hydrology, Faculty of Biology, Regional Campus of International Excellence 'Campus Mare Nostrum', University of Murcia, 30100 Murcia, Spain

ABSTRACT: A Monitoring-PAM fluorometer with high temporal resolution (every 5 min) was used to assess the effects on photosynthesis in *Ulva rigida* (Chlorophyta) during exposure to 2 different CO_2 conditions: current ('LC', 390 ppm), and the predicted level for the year 2100 ('HC', 700 ppm) in a crossed combination with 2 different daily pulsed nitrate concentrations ('LN', 5 µM and 'HN', 50 µM) and 2 temperature regimes (ambient and ambient +4°C). Effective quantum yield ($\Delta F/F_m'$) in the afternoon was lower under HCLN conditions than under the other treatments. The decrease in $\Delta F/F_m'$ from noon to the afternoon was significantly lower under +4°C compared to ambient temperature. Maximal quantum yield (F_v/F_m) decreased during the night with a transient increase 1 to 3 h after sunset, whereas a transient increase in $\Delta F/F_m'$ was observed after sunrise. These transient increases have been related to activation/deactivation of the electron transport rate and the relaxation of non-photochemical quenching. Relative electron transport rate was higher under the LC and +4°C treatment, but the differences were not significant due to high variability in daily irradiances. Redundancy analysis on the data matrix for the light periods indicates that photosynthetically active radiation through the day is the main variable determining the physiological responses. The effects of nutrient levels (mainly carbon) and experimental increase of temperature were low but significant. During the night, the effect of nutrient availability is of special importance with an opposite effect of nitrogen compared to carbon increase. The application of the Monitoring-PAM to evaluate the effects of environmental conditions by simulating climate change variations under outdoor-controlled, semi-controlled conditions is discussed.

KEY WORDS: Climate change · *In vivo* chlorophyll fluorescence · Monitoring-PAM · Nitrate · Ocean acidification · Temperature · *Ulva rigida*

INTRODUCTION

A significant fraction of the anthropogenically-produced CO_2 released into the atmosphere has been taken up by the oceans since the last century, causing various impacts on photosynthetic activity (Riebesell et al. 2007, Doney et al. 2009, Raven 2011). Continuous dissolution of CO_2 from the atmosphere

*Corresponding author: felix_lopez@uma.es

Publisher: Inter-Research · www.int-res.com

into the oceans has led to an increase in ocean surface acidification by 0.1 pH unit (corresponding to a 30% increase of H^+) since 1800. In addition, atmospheric CO_2 levels are expected to rise under the 'business-as-usual' CO_2 emission scenario (Brewer 1997), which could result in further ocean acidification (OA) by 0.3 to 0.4 units (about a 100 to 150% increase of H^+) by 2100 (Caldeira & Wickett 2003). The awareness of the magnitude of these changes at a global level has led to a recent surge in research efforts to increase our understanding of OA impacts not only on ocean chemistry (Pelejero et al. 2011), but also on biology (Roleda & Hurd 2012).

Studies on the ecological and physiological impacts of elevated CO_2 concentrations in macroalgae were initiated in the early 1990s (Gao et al. 1993). Since then, investigations that mainly focused on isolated impacts of CO_2 levels have revealed mixed, and at times contradicting responses, depending on the species examined and the culture conditions applied (Hurd et al. 2009). Therefore, an analysis of the responses of different algal groups to OA can be expected to be complex, due to the interactive effects of pH and CO_2 on different physiological processes (Mercado 2008). Calcifying algae, which seem to be particularly sensitive to reduced water pH, have been the focus of several studies (Martin & Gattuso 2009, Russell & Connell 2012). By contrast, non-calcareous species have received much less attention, resulting in a significant gap in our knowledge despite the likely accumulative effects (Harley et al. 2012).

In this study, we analyzed the effects of C, N and temperature treatments on photosynthetic activity. *In vivo* chlorophyll fluorescence has been extensively applied in macroalgal eco-physiology to estimate photosynthetic efficiency and capacity (Schreiber & Bilger 1993, Figueroa et al. 1997, Beer et al. 2000, Nitschke et al. 2012). Effective quantum yield ($\Delta F/F_m'$) is used as an indicator of acclimation of photosystem II (PSII), whereas the maximal quantum yield (F_v/F_m) is used as an indicator of photoinhibition, and the electron transport rate (ETR) as a proxy of photosynthetic capacity or productivity (Figueroa et al. 2013). Recently, a new chlorophyll fluorometer, commercially known as Monitoring-PAM (Walz), has been designed for autonomous, long-term monitoring of chlorophyll fluorescence under field conditions. The monitoring of photosynthetic yields of aquatic species over full daily cycles *in situ* with a high temporal resolution has been achieved in ice algal communities by using a Monitoring-PAM (McMinn et al. 2003), or by using a submersible fluorometer (Aquation) in tropical seagrasses such as *Halophila stipulacea* (Runcie et al. 2009). Similarly, a Monitoring-PAM has previously been applied to vascular species in the Arctic (Barták et al. 2012), and a Monitoring-PAM data acquisition systems (Moni-DA, Gademann Instruments) to natural soil crusts in deserts dominated by lichens and cyanobacteria (Raggio et al. 2014). In addition, high-resolution chlorophyll fluorescence has been monitored in mesocosms in the microalgae *Chlorella fusca* growing in thin-layer cascades by using a Junior-PAM fluorometer (Figueroa et al. 2013).

The Monitoring-PAM fluorometer allows the determination of $\Delta F/F_m'$ and irradiance at a high temporal resolution scale (minutes) within experimental mesocosms (as a non-intrusive approach). On the other hand, the monitoring of maximal fluorescence (F_m') and F_t (actual fluorescence in actinic light prior to applying the saturation pulse) can provide information on photo-physiological acclimation. An increase of F_t with increasing irradiance is related to inactivation of PSII: i.e. closure of the PSII reaction center, reduction of the electron sink and a decrease of CO_2 fixation (Ralph & Gademann 2005). In addition, photosynthetic yield can also be monitored during the night, adding information to this poorly-understood part of the daily cycle.

Within the framework of the 9th International Workshop on Aquatic Primary Productivity (GAP) hosted by the University of Malaga (southern Spain), we used outdoor mesocosms (for a detailed description see Stengel et al. 2014, this Theme Section), to analyse the effects of current pCO_2 (LC, 380 ppm) and the concentration predicted for the year 2100 (HC, 700 ppm) (Orr et al. 2005, Meehl et al. 2007) in a crossed combination with 2 daily pulsed nitrate concentrations: 5 µM (LN) and 50 µM (HN). The LN level of nitrate is near the high end of the natural range of concentrations in the local area at the time of the year when the experiment was conducted (Ramírez et al. 2005); thus, the LCLN treatment can be considered a control, as it was closest to the natural conditions. Additionally, the effects of a short-term temperature increase (+4°C) on photosynthetic activity in *Ulva rigida* (Chlorophyta) were assessed. Using a Monitoring-PAM fluorometer, this study aimed to analyse the high-resolution photosynthetic responses (chlorophyll fluorescence) of *U. rigida* to carbon, nitrogen and temperature as described above, and detailed in Stengel et al. (2014). To our knowledge, this is the first time that this equipment was utilized to continuously monitor macroalgal photosynthetic performance.

MATERIALS AND METHODS

Species and experimental design

Samples of *Ulva rigida* C. Agardh (Chlorophyta) were collected in La Araña (36° 45′ N, 4° 18′ W) at the coast of Malaga (Alboran Sea, southern Iberian Peninsula) on 9 September 2012. Samples were transported in a cool box to the laboratory and maintained under LCLN conditions (after removing any visible epibiota) for an acclimation period of 5 d (until 14 September). Subsequently, the experimental conditions of the different treatments (i.e. LCLN, HCLN, LCHN, HCHN) under ambient temperature (19°C) were established and algae were allowed to grow for a period of 6 d (from 15 to 20 September) before the temperature was raised by 4°C for 3 additional days (from 21 to 23 September). Details of the experimental design, as well as the monitoring of environmental parameters throughout the experiment are described in Stengel et al. (2014). Each sample holder was positioned in the treatment vessels (one head per treatment) (Fig. 1A), which contained other *U. rigida* thalli used for different measurements and analyses (Figueroa et al. 2014, this Theme Section, Stengel et al. 2014). Although the sample holder was positioned very close to the water surface, other floating *Ulva* thalli could not be prevented from passing over the sensor, causing some temporal shading. In order to solve this problem, the sample holder was isolated from the rest of the algae in the vessels by means of a small, open plastic mesh cage, which allowed the continuous exchange of water but prevented potential shading by other thalli (Fig. 1B). A piece of *U. rigida* sheet was fixed to the sample clip, which was mounted at a distance of 25 mm from the Moni-head/485 optical window (Fig. 1B), forming an angle of 45° between the holder and the sample. This position reduced shade areas in the sample and allowed for correct determination of $\Delta F/F_m'$ as described in the procedure of other PAM fluorometers (Schreiber & Bilger 1993).

In this study, we present the data from the evenings of 18 to 20 September (ambient temperature treatment) and 21 to 22 September (+4°C treatment). The temperature was increased between 19:00 and 20:00 h GMT (21:00 to 22:00 h local time). In this paper, the time is presented as GMT (i.e. 2 h earlier than local time).

In vivo chlorophyll *a* fluorescence

Measurements of *in vivo* chlorophyll fluorescence were recorded every 5 min, starting on Day 4 of the experiment using an aquatic version of the Monitoring-PAM fluorometer, hereafter referred to as Moni-PAM. A general technical description of the Moni-PAM system and its operation under field conditions is given in Porcar-Castell et al. (2008). The operating modes of the aquatic and terrestrial versions are similar, although external materials, connectors, and some calibration protocols allow the aquatic version to operate underwater. Our measuring system con-

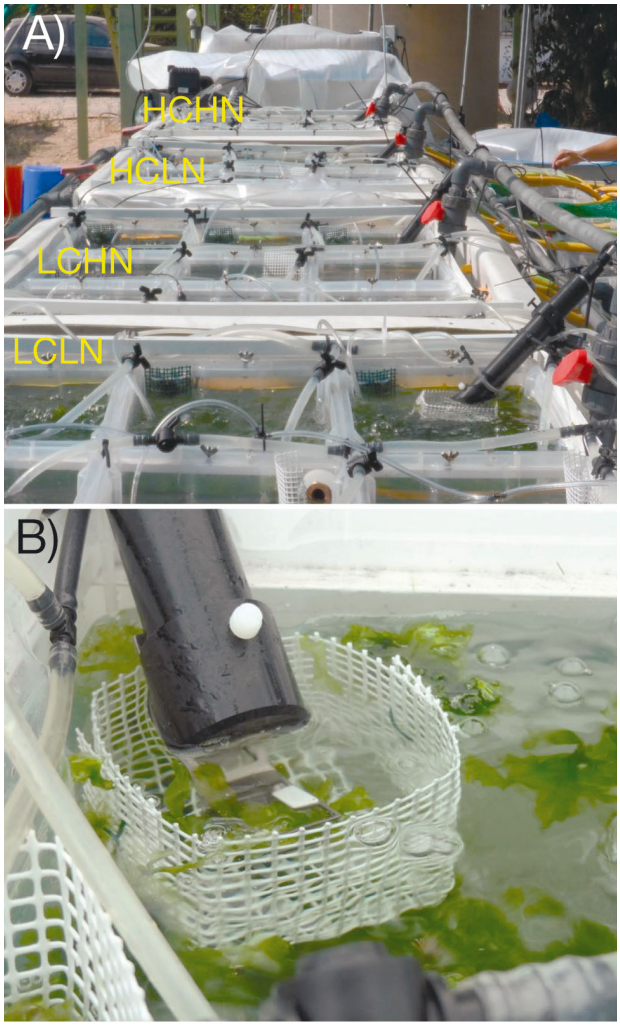

Fig. 1. (A) Experimental mesoscom setup showing the 18 l vessels containing *Ulva rigida* floating thalli used during the 9th GAP workshop. A Moni-head emitter-detector (black tubes on the right) is used in each vessel. Treatments consisted of 2 levels of pCO_2, i.e. unenriched air (low carbon, LC, 380 ppm) and air enriched with CO_2 (high carbon, HC, 700 ppm), and 2 different nitrate pulsed concentrations, i.e. high nitrate (HN, 50 µM) and low nitrate (LN, 5 µM), in the following combinations: LCLN, LCHN, HCLN and HCHN. (B) Moni-head emitter-detector unit beside the sample holder containing an *U. igida* disc inside the mesh box. The white laminar area conducts the reflected light to the incident irradiance (E_{PAR}) sensor located inside the Moni-head

sisted of 4 emitter-detector units (Moni-head/485) connected to a data acquisition system (Moni-DA) by 10 m long cables.

During the night, F_v/F_m was determined every 5 min, where $F_v = F_m - F_0$; F_m is the maximal fluorescence after a saturation pulse and F_0 is the basal fluorescence of fully oxidized reaction centers. In order to avoid excitation of chlorophyll by repetitive pulses of the measuring light, the light was switched off between measurements (each 5 min) but automatically switched on a few seconds before each saturating-pulse analysis using the batch file feature of the WinControl-3 software. In a previous experiment, it had been demonstrated that 5 min of darkness is enough to reach full oxidation of reaction centers since no significant differences in the F_v/F_m values were observed compared to 15 or 30 min dark incubation (data not shown). Thus during the night, true F_0 and F_m were measured using 5 min dark periods between measurements.

During the light period, $\Delta F/F_m'$ was determined every 5 min, where $\Delta F = F_m' - F_t$; F_m' is the maximum fluorescence yield of an illuminated sample and F_t is the instantaneous fluorescence of illuminated algae measured briefly before application of a saturation pulse. Values of F_m' were recorded after applying saturating pulses provided by blue light-emitting diodes (LEDs). The same blue LED emits actinic and saturating flashes as well as measuring light; the LED emission maximum and full width at half maximum is 455 nm and 18 nm, respectively. The intensity of the measuring light to determine F_0 and F_t was 0.9 µmol photons m^{-2} s^{-1} and 9 µmol photons m^{-2} s^{-1} at F_m, and the intensity of saturating pulses was 4000 µmol photons m^{-2} s^{-1}.

The relative electron transport rate through PSII (rETR), expressed as µmol electrons m^{-2} s^{-1} was determined as follows:

$$rETR = \Delta F/F_m' \times E_{PAR} \quad (1)$$

where E_{PAR} is the incident irradiance of photosynthetically active radiation (PAR, from 400 to 700 nm) expressed in µmol photons m^{-2} s^{-1}. The irradiance was monitored by using a PAR quantum sensor inserted in the Moni-PAM fluorometer. This sensor measures the radiation reflected by a 1.3 × 0.7 cm area of an optically diffuse Teflon sheet mounted at the edge of the leaf clip (Fig. 1B). Daily irradiance data under LCLN and HCLN treatments are presented.

The photosynthetic parameters maximal relative electron transport rate ($rETR_{max}$), saturated irradiance (E_k) and photosynthetic efficiency (α_{ETR}) were calculated by exponential fitting of the function rETR versus irradiance according to Webb et al. (1974).

The relationship between $\Delta F/F_m'$ and E_{PAR} was analysed separately for the morning and afternoon periods by fitting $\Delta F/F_m'$ versus E_{PAR} curves to an exponential decay function following Ritchie (2008):

$$\Delta F/F_m' = \Delta F/F_{m'max} \times e^{-k \times E_{PAR}} \quad (2)$$

where $\Delta F/F_{m'max}$ is the effective quantum yield at theoretical zero irradiance, k is a constant and E_{PAR} is the irradiance.

Statistical analyses

To allow for statistical evaluation, data from the first and second experimental days (19 and 20 September) were considered as replicates of the ambient temperature condition, and the data from the third and fourth experimental days (21 and 22 September) were considered as replicates of the increased temperature (+4°C). Data were treated as 2 replicates (n = 2); subsequently, a 2-way ANOVA was applied using SPSS v.21 software (IBM), with temperature (with or without the 4°C increment), and treatments (LCLN, LCHN, HCLN, and HCHN) as factors. The following dependent variables were evaluated: rETR integrals, $rETR_{max}$, α_{ETR}, E_k; with respect to daily yield variation, $\Delta F/F_{m'max}$ and the constant k were considered in the morning and afternoon periods separately. Student-Newman-Keuls tests (SNK) were performed after significant ($p < 0.05$) ANOVA interactions (Underwood 1997). If no interaction between 2 factors were found, the data were pooled and the significance of the new combination of data was evaluated (Martínez et al. 2012). The effect of treatment on the nightly decrease of F_v/F_m was evaluated using a test that compared simple linear regression equations (Zar 2009). To analyze the multivariate response of photosynthetic variables to the different experimental conditions, we performed 2 redundancy analyses (RDA), the canonical form of the Principal Component Analyses, on the matrix of diurnal and nocturnal measurements. As photosynthesis variables, we considered F_m', F_t, $\Delta F/F_m'$ and rETR for the diurnal measurements, and F_m, F_0 and F_v/F_m for the night. As environmental variables, we considered temperature measured in the tanks, time of day (in h:min), PAR radiation, and nitrate and CO_2 concentration as dummy variables (low, high). The relative contribution of each variable to the ordination was evaluated with a Monte Carlo permutation test. All matrixes were previously square root transformed. Ordinations were performed using CANOCO v.4.1 software (Leps & Smilauer 2003).

RESULTS

During the first day of measurements, the incident irradiance reaching the algal thalli showed a high variability (Fig. 2A) with continuous and rapid changes, in contrast to the irradiance outside the vessels, which revealed a homogeneous pattern (see Stengel et al. 2014). In addition, the irradiance data also showed differences between treatments throughout the first day. The irradiance reaching the algae sample within each treatment varied slightly according to shaded short episodes produced by algae located on the optically neutral Teflon sheet. Thus, the daily dose of E_{PAR} received by the samples under each carbon and nutrient treatment was not identical (Fig. 2A). For example, on the second day (20 September), the samples under the LCLN treatment received the highest daily dose of E_{PAR} while the samples under the HCHN treatment received the lowest daily integrated irradiance (data not shown), whereas on the morning of the last day (22 September), the irradiance under HCLN was higher than that under LCLN (Fig. 2A). On this day, the sample that received the highest dose was the sample under HCHN, while the lowest radiation corresponded to the sample under HCLN (data not shown). Temperatures were well controlled and followed the expected variation during the experimental period (Fig. 2B, showing LCLN and HCLN treatments; the other 2 treatments followed the same pattern but are not presented to highlight temperature variation), ensuring that samples were exposed to the 4°C average increment on the last 3 experimental days.

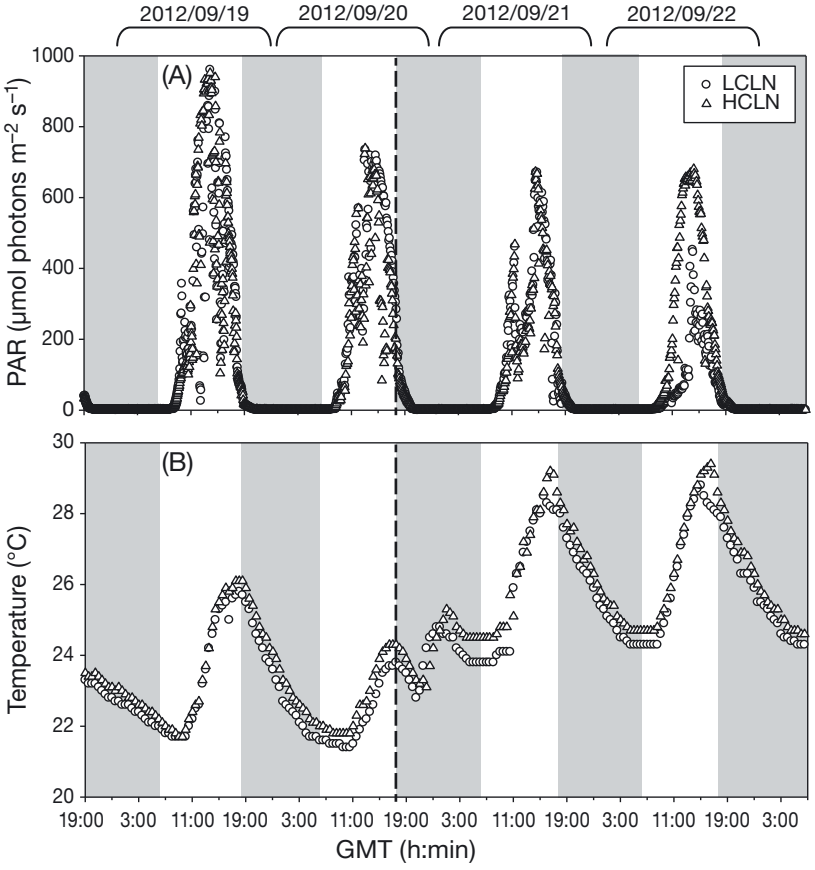

Fig. 2. Abiotic parameters variation against experimental period in GMT of cultivation of *Ulva rigida* subjected to 2 conditions of CO_2 supply and 2 different nitrate pulsed concentrations (see Fig. 1 for description of treatment conditions) under ambient temperature for 2 d (19 and 20 September 2012). After this period, temperature was increased (+4°C) under the same carbon and nitrate treatments for another 2 d (21 and 22 September 2012). (A) Irradiance variations during the experimental period. PAR: photosynthetically active radiation (400–700 nm). Gray background indicates dark periods. (B) Temperature variation during experimental period. Dashed line indicates when the temperature was increased. Both (A) and (B) panels represent only LCLN and HCLN treatments to allow for clarity. The other 2 treatments (LCHN and HCHN) followed the same pattern (data not shown)

The variations of F_m' and F_t (light periods) and F_m and F_0 (night periods) of LCLN and HCLN are presented in Fig. 3A,B. Under LCLN and ambient temperature, on the first 2 nights (18–19 and 19–20 September), F_m increased from sunset to 22:30 h and then decreased to sunrise, whereas F_0 slightly increased during the night (Fig. 3A). On the second night (20 September), F_m increased from sunset to 23:30 h GMT and then decreased until sunrise (06:03 h GMT). F_0 presented a similar pattern as F_m but the slopes of increase and decrease were lower than that of F_m. During the light period, F_m' and F_t changed in the same manner, with a decrease through the day. F_m' and F_t decreased from morning until noon, and then increased in the afternoon and in the early night as described above (Fig. 3A). In addition, on 19 September a transient increase of both F_m' and F_t was observed on 13:00 h GMT. This transient increase was also observed in the following day, but at 15:00 h GMT. At the increased temperature (+4°C treatment) the values of either F_m or F_m' and F_0 or F_t were higher than those under ambient temperature (Fig. 3A). In the beginning of the experiment, the night peak occurred at 19:30 whereas on the next experimental days it occurred before or close to 23:00 h (Fig. 3A). On 20 September at 20:00 h GMT there was a drastic increase in F_m until 22:30 h, and then a

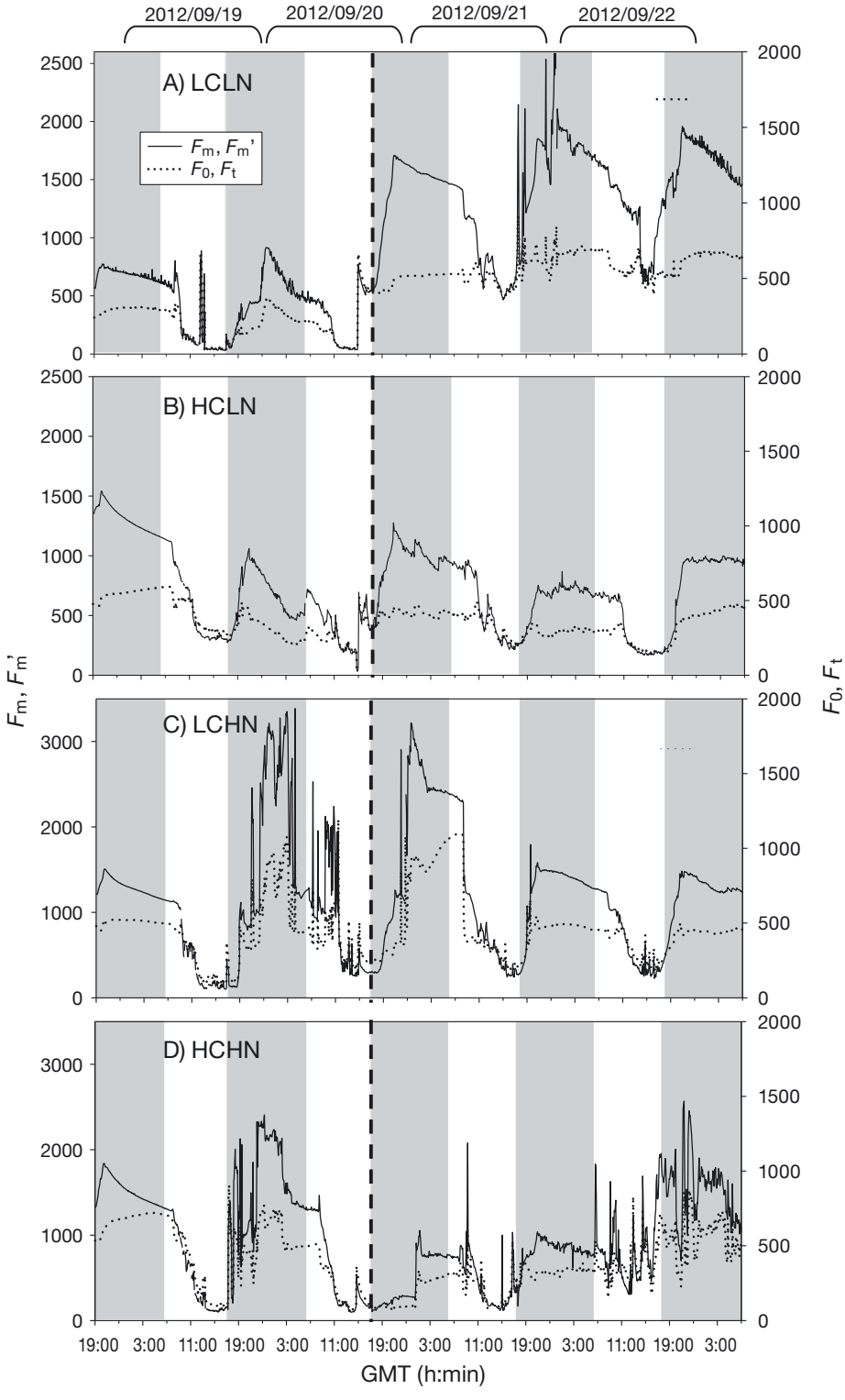

Fig. 3. Variation of fluorescence responses of *Ulva rigida* against experimental period in GMT, subjected to 2 conditions of CO_2 supply and 2 different nitrate pulsed concentrations (see Fig. 1 for description of treatment conditions) under ambient temperature for 2 d (19 and 20 September 2012). After this period, temperature was increased (+4°C) under the same carbon and nitrate treatments for another 2 d (21 and 22 September). Dashed line indicates when temperature was increased. Fluorescence parameters — dark periods (shaded gray): F_0 = basal fluorescence, F_m = maximal fluorescence after a saturation pulse; light periods: F_t = instantaneous fluorescence, F_m' = maximum fluorescence yield. Solid line: F_m, F_m'; dotted line: F_0, F_t. (A) LCLN; (B) LCHN; (C) HCLN; (D) HCHN

decrease until sunrise. On the other hand, in the +4°C treatment, F_m' and F_t changed in the same manner over a short period (i.e. from 15:00 to 17:00 h GMT).

At HCLN, only mariginal differences in F_m or F_m' and F_0 or F_t were observed for the 2 temperature treatments (Fig. 3B). In contrast to LCLN, the patterns of the maximal F_m and F_0 in the night were similar, i.e. a decrease was observed 2 to 3 h after sunset in all C–N treatments, except for the first 2 nights (18–19 and 19–20 September), when F_m decreased and F_0 increased. During the light period, maximal values F_m' and F_t appeared about 1 h after sunrise at ambient temperature, whereas at +4°C, maximal values were observed 3 to 4 h after sunrise. Under the increased temperature treatment, F_m' and F_t changed in the same manner from 11:00 h to sunset (about 18:15 h GMT).

Fluorescence parameters under LCHN and ambient temperature presented a similar pattern but with higher F_m and F_0 values than that observed under LCLN (Fig. 3C). Maximal values of F_m and F_t appeared 3 to 5 h after sunset under ambient temperature and 2 to 4 h after sunset under +4°C. At the increased temperature, the F_m' increase was much lower than that under LCLN (Fig. 3A). The differences between F_m and F_0 were much lower than that under LCLN. F_m' and F_t are coupled in the light period from 13:00 to 19:00 h under both temperature treatments (Fig. 3C). Finally, under HCHN treatments the pattern of fluorescence parameters (Fig. 3D) were similar as under HCLN (Fig. 3B), but with maximal values 3 to 4 h after sunrise. However, during the +4°C treatment, values of F_m' and F_t were higher than that under HCLN (Fig. 3B,D). The maximal values of F_m and F_0 observed during the night appeared 2.5 h after sunset. F_m' and F_t changed in the same manner in the light period from 11:00 h to sunset (18:15 h) (Fig. 3D). Maximal

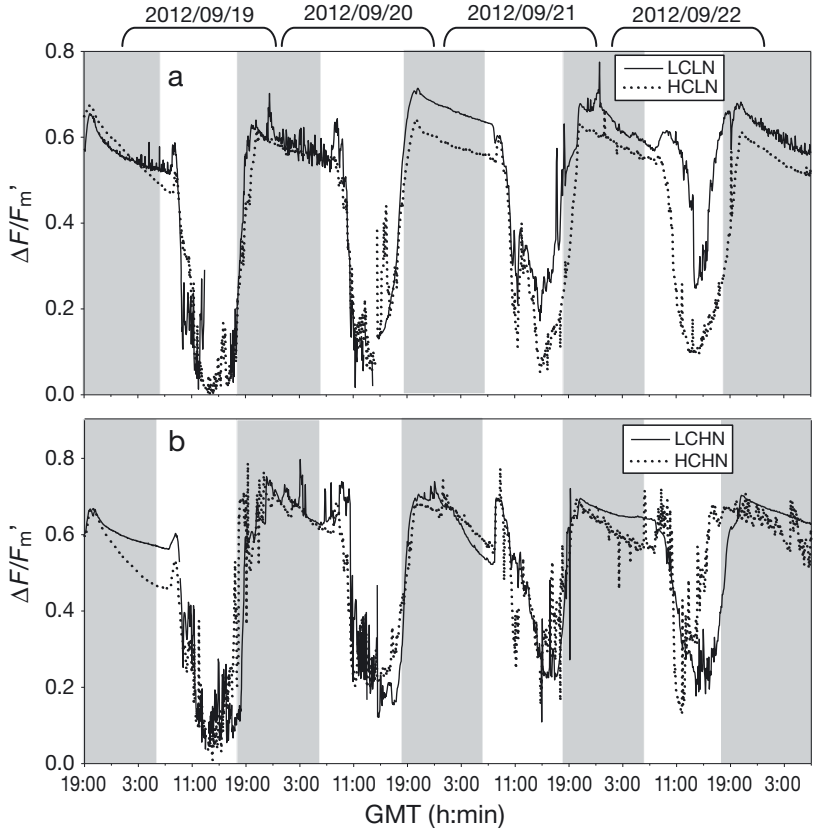

Fig. 4. Variation of effective quantum yield ($\Delta F/F_m'$) of *Ulva rigida* against experimental period in GMT, subjected to 2 conditions of CO_2 supply and 2 different nitrate pulsed concentration (see Fig. 1 for description of treatment conditions) under ambient temperature for 2 d (19 and 20 September 2012). After this period, temperature was increased (+4°C) under the same carbon and nitrate treatments for another 2 d (21 and 22 September 2012). Gray background indicates periods of darkness. (A) LCLN and HCLN treatments; (B) HCLN and HCHN treatments

values of F_m' and F_t under ambient temperature were observed 0.5 to 2 h after sunrise, whereas at +4°C the maximal values occurred after 3 h (Fig. 3D).

The variation in F_v/F_m during the night period (Fig. 4) as a consequence of the variation in F_m and F_0 can be analyzed as changes in the negative slopes of the function F_v/F_m versus time (Table 1). During the night of 18–19 September, the decrease of F_v/F_m was about 3 times higher under HC than that under LC, regardless of N conditions. During the night of 19–20 September, the decrease of F_v/F_m was higher under HN treatments (HCHN and LCHN) than under LCLN, followed by HCLN. In the following night (20–21 September) under increased temperature, the slopes of decrease in F_v/F_m were greater than those during the previous night, except for LCLN (Table 1). This decrease was higher again under HN (LCHN followed by HCHN) than in the LN treatments. During the second night after the temperature increase (21–22 September), the slopes of decrease in F_v/F_m were lower than during the previous night. In addition, on 21–22 September, the largest decrease was observed under LCLN, followed by HCLN and HCHN, and the smallest decrease occurred under LCHN. During the last night under increased temperature (22–23 September), again, the steeper slopes were observed under the LN treatment but also under HCHN, and again, the smallest decrease occurred under LCHN.

The $\Delta F/F_m'$ presented a typical daily pattern, with a decrease from the morning to about noon, followed by an increase until sunset. Interestingly, $\Delta F/F_m'$ presented a transient increase in the morning, about 1 to 3 h after sunrise. During the night, F_v/F_m also presented a transient increase about 1 to 3 h after sunset. For most of the experimental period, $\Delta F/F_m'$ was higher under the LCLN than the HCLN treatment (Fig. 4A). On the other hand, $\Delta F/F_m'$ was slightly higher under LCHN than that under HCHN (Fig. 4B). However, according to the curve-fitted

Table 1. Slopes ± SE of the effective quantum yield nighttime variation under the different nitrate and CO_2 treatments, calculated using a test for comparing simple linear regression equations (see Fig. 1 for description of treatment conditions). Different superscripted letters indicate significant ($p < 0.05$) differences. The nights of 18–19 and 19–20 September correspond to ambient temperature, whereas the nights of 20–21, 21–22 and 22–23 September correspond to ambient temperature increased by 4°C

Treatment	Ambient temperature				Ambient temperature +4°C					
	18–19 Sep		19–20 Sep		20–21 Sep		21–22 Sep		22–23 Sep	
	Slope	R^2	Slope	R^2	Slope	R^2	Slope	R^2	Slope	R^2
LCLN	-0.117 ± 0.001^{a}	0.571	-0.154 ± 0.021^{cb}	0.378	-0.139 ± 0.001^{b}	0.991	-0.271 ± 0.008^{e}	0.932	-0.216 ± 0.009^{ce}	0.862
LCHN	-0.126 ± 0.001^{a}	0.987	-0.206 ± 0.025^{ce}	0.427	-0.565 ± 0.009^{f}	0.978	-0.064 ± 0.002^{d}	0.889	-0.152 ± 0.002^{bc}	0.988
HCLN	-0.357 ± 0.002^{g}	0.997	-0.087 ± 0.005^{d}	0.782	-0.128 ± 0.003^{a}	0.964	-0.192 ± 0.009^{cb}	0.825	-0.211 ± 0.004^{ce}	0.962
HCHN	-0.345 ± 0.005^{g}	0.997	-0.248 ± 0.007^{e}	0.784	-0.424 ± 0.010^{h}	0.951	-0.175 ± 0.022^{b}	0.413	-0.286 ± 0.025^{e}	0.580

Table 2. Two-way ANOVA representing effects of 2 factors (temperature and treatment) and their interaction on different dependent variables measured in *Ulva rigida* during the 4 d experimental period (first 2 d at ambient temperature, next 2 d increased by 4°C). Temperature was increased at the sunset of the second experimental day (20 September). Temperatures: ambient, ambient +4°C; treatments: LCLN, LCHN, HCLN and HCHN (see Fig. 1 for description of treatment conditions). Significant values (at $p < 0.05$) are in **bold**. n = 2

Variable	Factor	df	MS	*F*	p
$\Delta F/F_m'$ morning period					
$\Delta F/F_{m'max}$	Temperature	1	0.0045	1.1727	0.3104
	Treatment	3	0.0064	1.6713	0.2494
	Temperature × Treatment	3	0.0014	0.3613	0.7828
	Residual	8	0.0038		
k	Temperature	1	0.0000	3.1073	0.1160
	Treatment	3	0.0000	0.7699	0.5425
	Temperature × Treatment	3	0.0000	0.5787	0.6452
	Residual	8	0.0000		
$\Delta F/F_m'$ afternoon period					
$\Delta F/F_{m'max}$	Temperature	1	0.0046	0.5470	0.4807
	Treatment	3	**0.0381**	**4.5124**	**0.0392**
	Temperature × Treatment	3	0.0060	0.7087	0.5734
	Residual	8	0.0085		
k	Temperature	1	**0.0000**	**14.5433**	**0.0051**
	Treatment	3	0.0000	0.2067	0.8889
	Temperature × Treatment	3	0.0000	0.2003	0.8933
	Residual	8	0.0000		
rETR					
Integrals	Temperature	1	1.08E+12	2.4789	0.1540
	Treatment	3	5.36E+11	1.2340	0.3593
	Temperature × Treatment	3	1.65E+11	0.3787	0.7711
	Residual	8	4.35E+11		
$rETR_{max}$	Temperature	1	2166.7861	1.4310	0.3039
	Treatment	3	7163.4218	4.7310	0.0613
	Temperature × Treatment	3	587.8399	0.3882	0.7647
	Residual	8	1514.1361		
α_{ETR}	Temperature	1	0.0098	0.6111	0.6266
	Treatment	3	0.0009	0.0534	0.8231
	Temperature × Treatment	3	0.0323	2.0233	0.1893
	Residual	8	0.0160		
E_k	Temperature	1	7278.2704	0.7081	0.5737
	Treatment	3	21170.3958	2.0597	0.1892
	Temperature × Treatment	3	2655.9581	0.2584	0.8534
	Residual	8	10278.3504		

parameters and statistical analysis (ANOVA), the morning values of $\Delta F/F_{m'max}$ were not significantly different, either for temperature or C and N treatments (Table 2), whereas in the afternoon, $\Delta F/F_{m'max}$ values were significantly ($p < 0.05$) affected by C and N but not by temperature (Table 2). The afternoon, values of $\Delta F/F_{m'max}$ were pooled with the factor which could have significant results (i.e. C and N treatments) (Table 2). Maximal values of $\Delta F/F_m'$ were significantly ($p < 0.05$) lower under HCLN than under the other C–N treatments (Fig. 5A,B). On the other hand, the slope of the function $\Delta F/F_m'$ versus irradiance (k) from the morning to noon was not affected by temperature or C and N treatments (Table 2). However, the slope (k) in the afternoon was significantly affected by the temperature treatments (Table 2). Thus, the k data in the afternoon are pooled following the factor which could have significant results (i.e. temperature). k was significantly ($p < 0.05$) higher at ambient than at +4°C (Fig. 5C,D).

The rETR also exhibited a strong diurnal pattern under all experimental conditions (Fig. 6) and displayed differences between treatments. The lowest rETR values in all treatments were observed in the first day (19 September) with a clear depletion around noon (Fig. 6A,B). During the next days (20 and 21 September), an increase in rETR was observed under LCLN and HCLN (Fig. 6A), mainly on 21 September (LCLN), with oscillations related to the decrease in irradiance due to cloud cover. These oscillations in rETR were also observed in the LCHN and HCHN treatments (Fig. 6B). Maximal values of rETR were reached around 14:00 to 15:00 h GMT.

The integrated rETR in the different C–N treatments did not reveal significant differences between the 2 temperature treatments (Table 2). Integrated rETR was higher under the LC and increased temperature treatments (mainly under LCHN), but due to the high variability between days, no significant differences could be detected (Table 2).

In order to determine the photosynthetic parameters, rETR values were plotted against irradiance. To simplify the presentation of the results, only the figures of LCLN and HCLN under the 2 temperature treatments are shown (Fig. 7). Typical photosynthetic curves were observed with more dispersion of data under ambient temperature (Fig. 7A,C) than under +4°C temperature (Fig. 7B,D). $rETR_{max}$ was higher under +4°C than under ambient temperature mainly in the LC treatments (Table 3) although these were not significant due to the high variability of the data (Table 2). At ambient temperature, HCHN showed the lowest

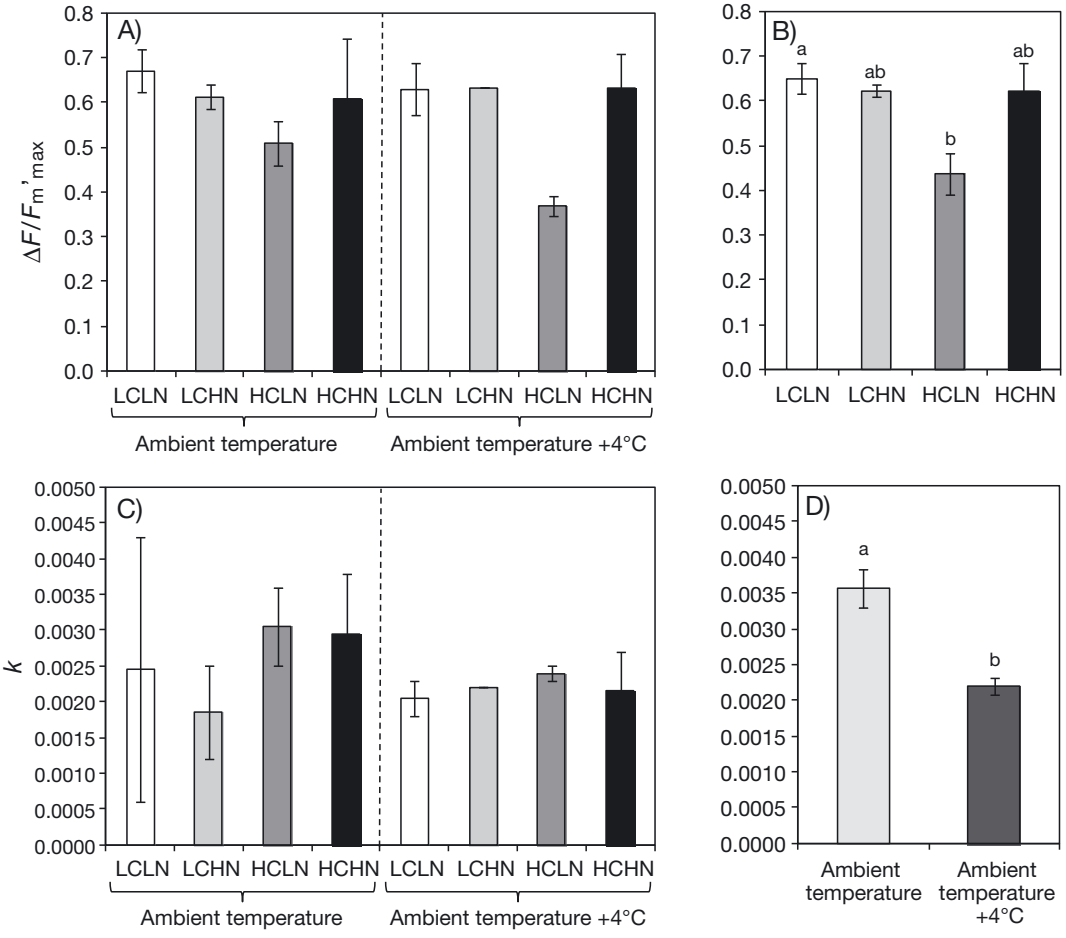

Fig. 5. Photosynthetic parameters ($\Delta F/F_m'_{max}$ and k) from effective quantum yield daily variation of *Ulva rigida* fitted to exponential decay function (Ritchie 2008). These values were calculated from algae submitted to 2 conditions of CO_2 supply and 2 different nitrate pulsed concentrations (see Fig. 1 for description of treatment conditions) under ambient temperature for 2 d (19 and 20 September 2012). After this period, temperature was increased (+4°C) under the same carbon and nitrate treatments for another 2 d (21 and 22 September 2012). These panels represent only conditions where significant factor effects were detected (see Table 2). Bars are means ± SE; different letters indicate statistically significant ($p < 0.05$) differences. (A) Values of $\Delta F/F_m'_{max}$ for the afternoon period (n = 2); (B) pooled data of $\Delta F/F_m'_{max}$ indicating differences amongst treatments (LCLN, LCHN, HCLN and HCHN). (n = 4); (C) values of constant k in the afternoon period (n = 2); (D) pooled k data showing differences between the 2 temperature conditions. (n = 8)

α_{ETR}, whereas for increased temperature this was observed for HCLN but values were not significantly different (Table 2). Finally, E_k was higher in LC (both N treatments) and HCLN treatments at +4°C than at ambient temperature, but again, the differences were not significant due to the high variability.

The RDA performed on the photosynthesis and environmental data matrix confirms that PAR through the day was the main variable determining the photosynthetic response of the algae (Fig. 8). The first 2 axes account for 38.5% of the total variance of the photosynthetic variables and 100% of the photosynthetic variables–environment relationship. The first axis alone explains 37.5% of the total variance of the photosynthetic variables and 97.2% of the photosynthetic variables–environment relationship, and ordinates the samples according to their values in rETR in the positive part, as a response to high values of PAR ($p = 0.002$), and high values of $\Delta F/F_m'$, F_m' and F_t to a lesser extent, in the negative part, linked to low PAR irradiance. The effect of nutrient concentration (mainly carbon) and experimental increase of temperature on the photosynthetic response of algae was low but significant (temperature: $p = 0.01$; C: $p = 0.006$) and it is recorded through the second axis. It represents only 1.2% of the total variance of the photosynthetic variables and 3.1% of the photosynthetic variables–environment relationship. The positive part of this axis is determined by temperature, mainly associated with the experimental increase of

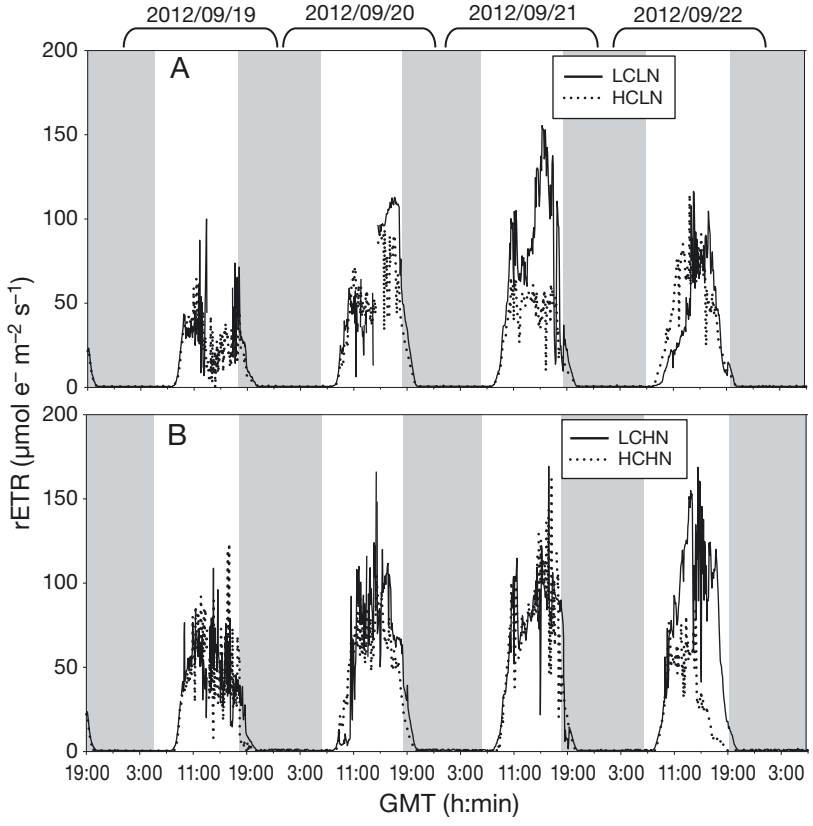

Fig. 6. Variation of relative electron transport rate (rETR) of *Ulva rigida* through time in GMT, subjected to 2 conditions of CO_2 supply and 2 different nitrate pulsed concentrations (see Fig. 1 for description of treatment conditions) under ambient temperature for 2 d (19 and 20 September 2012). After this period, temperature was increased (+4°C) under the same carbon and nitrate treatments for another 2 d (21 and 22 September 2012). Gray background indicates periods of darkness. (A) LCLN and HCLN treatments; (B) HCLN and HCHN treatments

4°C. Higher nitrogen concentrations also affected the positive part of this axis, but this was not significant (p = 0.1). The increase in temperature was associated mainly with an increase in rETR, a very small increase in F_t and a slight decrease in $\Delta F/F_m'$. The negative impact was determined by high C concentrations with a small influence on photosynthetic variables. The effect of increased temperature must be considered with caution, as in the experimental conditions this was also associated with changes in PAR (particularly at noon).

During the night, the effect of nutrient availability was important (Fig. 9). The first 2 axes of the RDA accounted for 20.7% of the total variance of the photosynthetic variables, and 100% of the relationship between photosynthetic variables and the environment. The first axis alone explained 20.6% of the total variance of the photosynthetic variables, and 99.6% of the photosynthetic variable–environment relationship. The positive part of this axis was associated with the highest values of all photosynthetic variables measured (F_m, F_0 and F_v/F_m). This axis was strongly linked with nutrient concentrations—with high N concentrations in the positive part and high C concentrations on the negative side (p = 0.005 in both cases). Temperature also had a significant influence on this axis (p = 0.005), separating the samples of the +4°C from the ambient temperatures in all nutrient treatments. PAR, which is also associated with this axis, was not significant (p = 0.56). Both low C concentrations (mainly when N was high) and increased temperature resulted in increases in F_m, F_0 and F_v/F_m, while high C concentrations tended to reduce them.

The second axis was associated with both temperature and time of day, separating the samples of the early night from the rest, and measurements at +4°C from those at ambient temperatures; however, time of day was not significant (p = 0.19). Increasing temperature tended to slightly increase F_v/F_m and decrease F_0.

DISCUSSION

The application of the Moni-PAM allowed for continuous monitoring of the instantaneous values of E_{PAR}, F_m' and F_t for the calculation of $\Delta F/F_m'$ during the light periods, and F_m and F_0 for the calculation of F_v/F_m during the dark, at high temporal resolution under experimental, outdoor conditions. In addition, simultaneous measurements of irradiance allowed the calculation of rETR.

The observations in a previous experiment that F_v/F_m was not significantly different after 5 min of dark incubation from that measured after 15 or 30 min supports the idea that F_v/F_m was correctly measured during darkness. Ihnken et al. (2010) found significant differences in *Ulva* sp. on rETR and $\Delta F/F_m'$ in the light after previous dark incubations of 15 compared to 95 min, which was similar to observations of different brown algae made by Nitschke et al. (2012). We were not able to determine F_v/F_m during the light period since no dark incubation could be applied. Runcie et al. (2009), by using a submersible fluorometer (Aquation) with an automated dark-acclimation function, found similar values for maximal fluorescence at midnight with various dark acclimation in

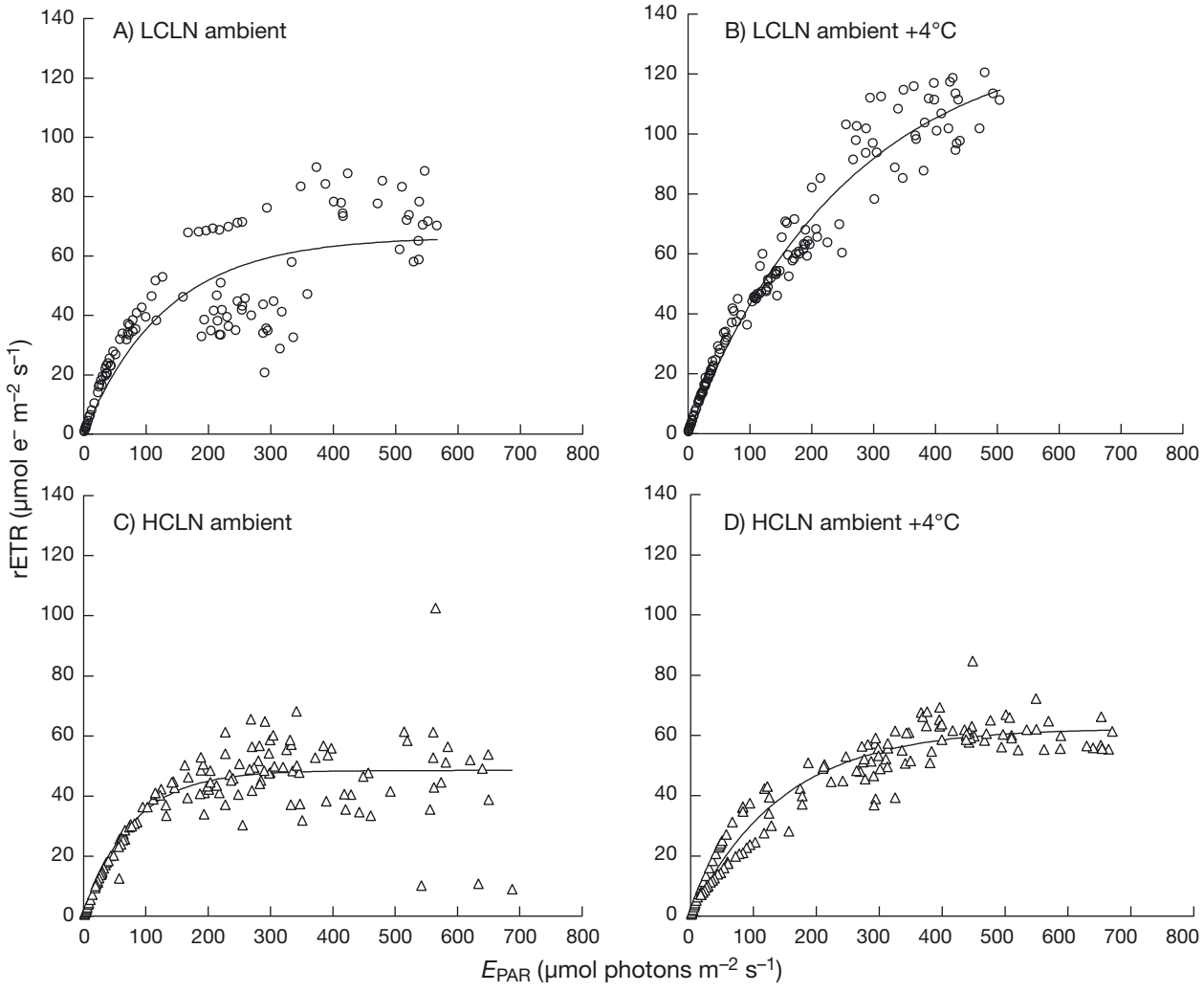

Fig. 7. Daily curves of relative electron transport rates (rETR, µmol electrons m^{-2} s^{-1}) against PAR irradiance (µmol photons m^{-2} s^{-1}) of *Ulva rigida*, subjected to 2 conditions of CO_2 supply and 2 different nitrate pulse concentration (see Fig. 1 for description of treatment conditions) under ambient temperature for 2 d (19 and 20 September 2012). After this period, temperature was increased (+4°C) under the same carbon and nitrate treatments for another 2 d (21 and 22 September 2012) (n = 2). (A) LCLN at ambient temperature; (B) LCLN at ambient temperature +4°C; (C) HCLN at ambient temperature; (D) HCLN at ambient temperature +4°C. Data were fitted to Webb et al. (1974) model, and photosynthetic parameters are presented in Table 3

Table 3. Photosynthetic parameters fitted from daily curves of relative electron transport rates (rETR) versus irradiance, applying the Webb et al. (1974) function in *Ulva rigida* for 2 d (19 and 20 September 2012) subjected to 2 conditions of CO_2 supply and 2 different nitrate pulsed concentrations (see Fig. 1 for description of treatment conditions) under ambient temperature. After the 2 d under the described bifactorial conditions, temperature was increased (+4°C) under the same carbon and nitrate treatments for another 2 d (21 to 22 September 2012). Maximal relative electron transport rates ($rETR_{max}$) are expressed as µmol electrons m^{-2} s^{-1}, and saturated irradiance (E_k) is expressed as µmol photons m^{-2} s^{-1}. α_{ETR} represents photosynthetic efficiency. Statistical analyses are presented in Table 2. Data are presented as means ± SE; n = 2, where each experimental day under the above described conditions was considered as a replicate

	Ambient temperature			Ambient temperature +4°C		
	$rETR_{max}$	α_{ETR}	E_k	$rETR_{max}$	α_{ETR}	E_k
LCLN	65.73 ± 24.54	0.54 ± 0.05	127.83 ± 57.33	133.23 ± 30.32	0.59 ± 0.12	245.46 ± 99.61
LCHN	72.17 ± 22.66	0.65 ± 0.05	115.09 ± 43.86	129.60 ± 26.81	0.67 ± 0.15	211.55 ± 85.71
HCLN	49.17 ± 14.98	0.69 ± 0.02	150.03 ± 24.37	64.64 ± 11.82	0.46 ± 0.08	190.03 ± 51.59
HCHN	93.70 ± 3.25	0.45 ± 0.05	211.04 ± 22.93	122.57 ± 54.12	0.65 ± 0.12	214.10 ± 31.03

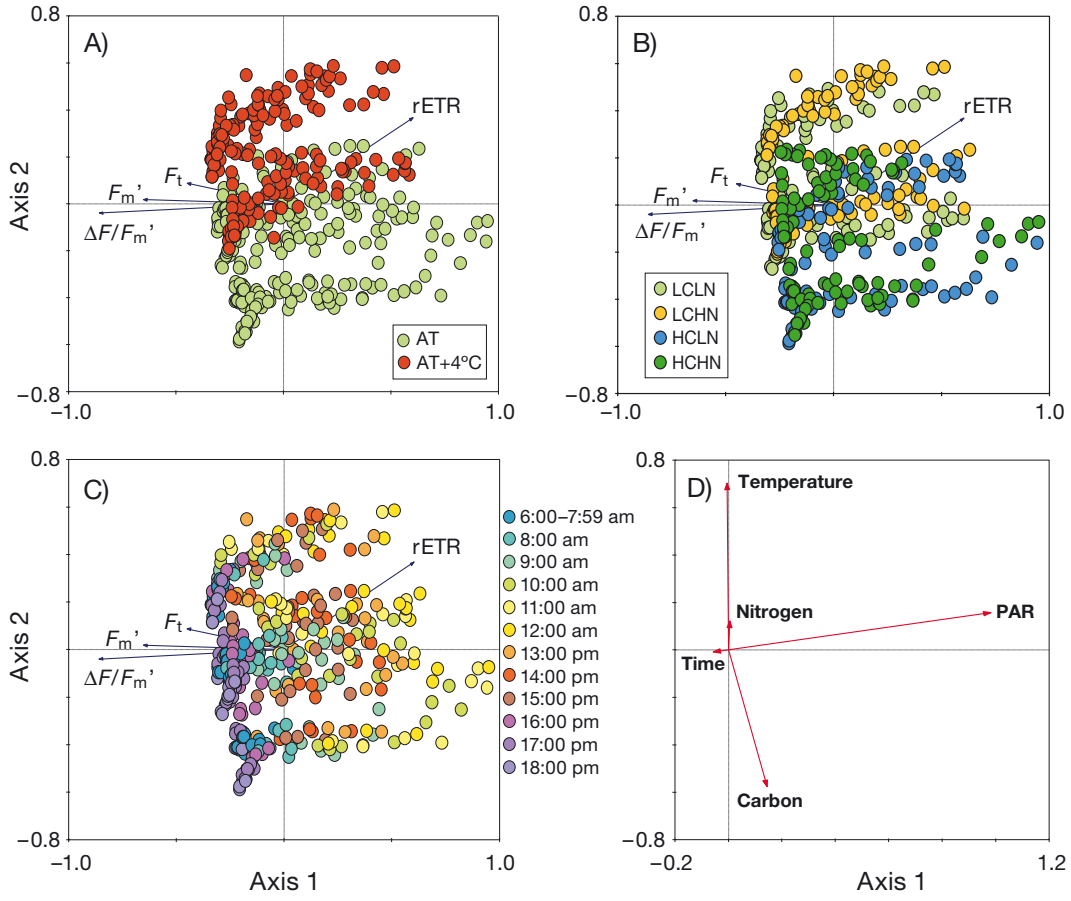

Fig. 8. Redundancy analysis (RDA) biplot ordination diagrams for fluorescence parameters and experimental conditions during the day, showing the main factors considered in the experiment. (A) Ambient temperature (AT) versus ambient temperature + 4°C; (B) nutrient concentration: HCHN, HCLN, LCHN and LCLN (see Fig. 1 for description of treatment conditions); (C) Time of day in 1 h intervals (except early morning, with 2 h intervals); (D) plot of the environmental variables on the ordination axes. PAR: photosynthetically active radiation. Fluorescence parameters (see Fig. 3 for F_m and F_t) — $\Delta F/F_m$': effective quantum yield; rETR: relative electron transport rate

the tropical seagrass *Halophila stipulacea*, regardless of the depth of the plant incubation (8, 12 or 33 m).

The physiological patterns observed in this study are discussed separately for the light and dark periods.

During the light periods

The effective quantum yield in the afternoon was significantly lower in HCLN compared to other treatments as also observed in studies using other fluorometers in similar experiments (*in situ* Diving-PAM, Stengel et al. 2014; PAM-2000 in the laboratory, Figueroa et al. 2014). Decreases in growth rate, maximal photosynthetic activity (as oxygen evolution), and nitrate reductase activity have been previously reported in *U. rigida* subjected to high CO_2 and low nitrate availability (Gordillo et al. 2001), as in this study under HCLN treatment. This was explained by a drastic decrease in absorptance due to the reduction of chlorophyll, and by increases in non-photochemical quenching and the excretion of dissolved organic carbon as energy dissipation mechanisms due to an imbalance of the C:N ratio (Gordillo et al. 2003). Although *U. rigida* is known to be carbon-saturated at current CO_2 concentrations (Mercado et al. 1998), it possesses a carbon-concentrating mechanism (CCM), a high affinity to take up CO_2 (Giordano et al. 2005, Raven et al. 2008) and an efficient mechanism to incorporate bicarbonate (Axelsson et al. 1995) at high pH, as occurred under LC treatments in the present study (see Stengel et al. 2014). *U. lactuca* was able to modify the seawater carbonate system via photosynthetic activity, and under pCO_2 of 280 ppm (preindustrial level), carbon acquisition was dependent on HCO_3^- uptake via an anion-exchanger (AE-state), the state with the highest affinity for HCO_3^- (Axelsson et al. 1995). In addition, the biomass of this species in-

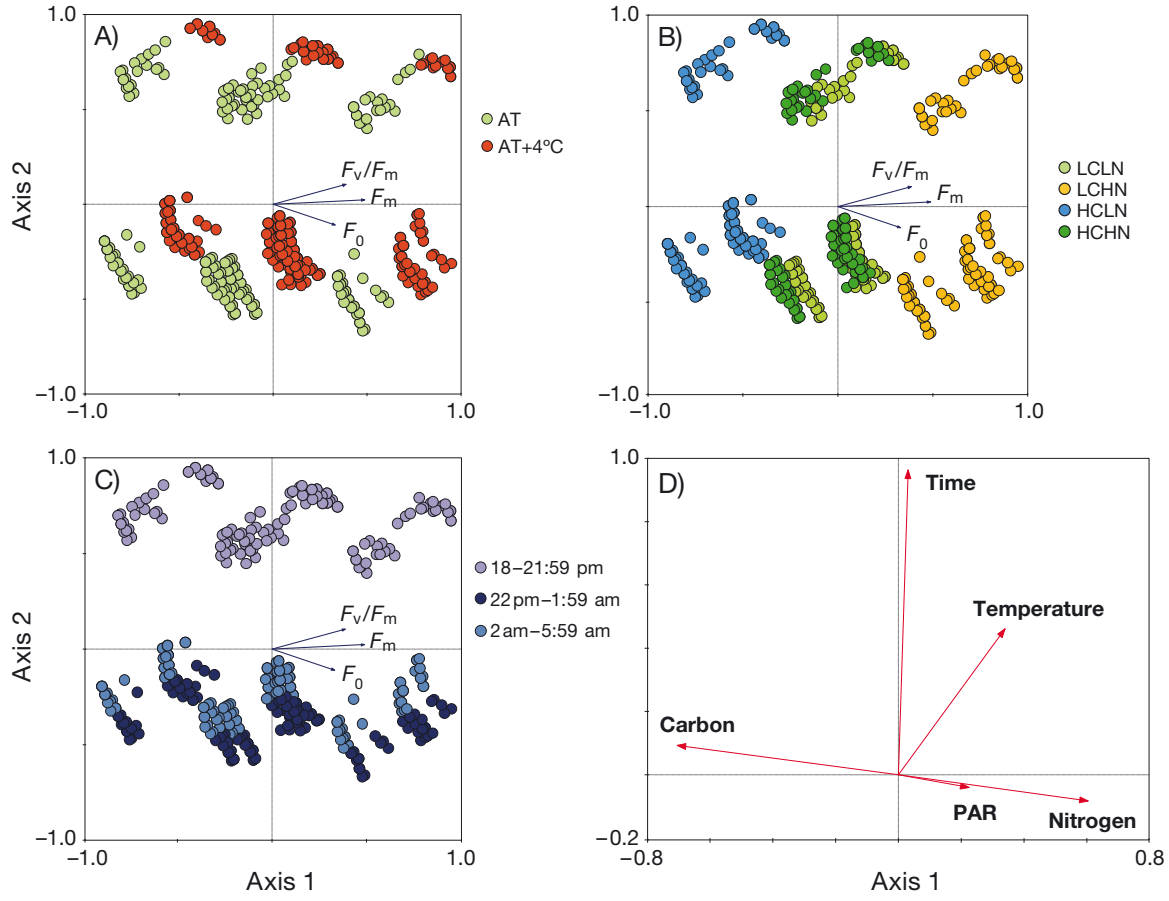

Fig. 9. Redundancy analysis (RDA) biplot ordination diagrams for fluorescence parameters and experimental conditions during the night, showing the main factors considered in the experiment. (A) Ambient temperature (AT) versus ambient temperature +4°C; (B) nutrient concentration: HCHN, HCLN, LCHN and LCLN (see Fig. 1 for description of treatment conditions); (C) time of day in 1 h intervals (except early morning, with 2 h intervals); (D) plot of the environmental variables on the ordination axes. PAR: photosynthetically active radiation. F_v/F_m: maximal quantum yield (other fluorescence parameters as in Figs. 3 & 8)

creased under the future scenario of increased CO_2 in rocky pools (Olischläger et al. 2013). In that study, the experimental design simulated the conditions of rocky pools since the algae were confined to a small volume, and the pH was increased due to photosynthetic activity (see Stengel et al. 2014). This is contrary to the general idea that macroalgae which have CCMs would be less sensitive to the predicted CO_2 level increases (Mercado 2008, Hepburn et al. 2011).

The slope of the decrease of effective quantum yield in the afternoon (k) can provide information on reversible adjustments of PSII to incident irradiance throughout the day, including short-time variations (for instance, temporary shading by clouds). Some differences between treatments on irradiance acclimation of PSII processes could be detected from the analysis of the $\Delta F/F_m'$ versus irradiance curves, both for the morning and afternoon measurements. In our study, k was higher under ambient temperature than under the +4°C treatment. A potential explanation for this observation could be that the temperature increase lead to an enhanced enzymatic reaction related to carbon or nitrogen assimilation as electron sinks (Pastenes & Horton 1996, Nishihara et al. 2005), hence causing a decrease in effective quantum yield as a consequence of the closure or reduction of reaction centers.

F_m' and F_t changes in the early morning produced transient increases in the effective quantum yields between 08:00 and 09:00 h (about 2 to 3 h after sunrise). These were followed by a drastic decrease in $\Delta F/F_m'$ due to increasing irradiance and the increase in energy dissipation as previously described for macroalgae (Enríquez & Borowitzka 2011). Such transient increases have been observed during *in situ* measurements in a terrestrial plant, *Pinus silvestris* (Porcar-Castell et al. 2008) and in the marine angiosperm *Halophila stipulacea* (Runcie et al. 2009).

The daily addition of 50 µM nitrate caused an increase in photosynthetic production compared to incubation under 5 µM. This is in agreement with the use of nitrate by this nitrophilic species, increasing the use of it as a sink of electrons due to the demand of ATP and NADPH for nitrate reduction to amino acids and proteins. The susceptibility to N availability has been reported both at photosynthetic and biochemical levels in *U. rigida* (Cabello-Pasini & Figueroa 2005, Figueroa et al. 2014). These data seem to indicate that a higher nitrate availability would be related not only to a slower decrease in energy efficiency throughout the morning but also to a greater capacity to process the energy available throughout the day, while CO_2 did not have an impact. A lower photosynthetic capacity, measured as ETR, and an early establishment of energy dissipation processes have already been documented for this species growing in the laboratory under N-limited conditions (Gordillo et al. 2003, Cabello-Pasini & Figueroa 2005). N-limitation affects different processes, such as photosynthetic capacity (Pérez-Lloréns et al. 1996) and photoprotection mechanisms (Korbee et al. 2005, Huovinen et al. 2006), but also induces changes in some cellular components, such as chlorophyll (Cabello-Pasini & Figueroa 2005), proteins (Henley et al. 1991, Vergara et al. 1995), and carbohydrates (Marek et al. 1995).

Over the diurnal cycle, F_t and F_m' provided information on the functioning of the rapid acclimation processes of energy partitioning in PSII. The term 'photosynthetic control' describes the short- and long-term mechanisms that regulate reactions in the photosynthetic electron transport (PET) chain so that the rate of production of ATP and NADPH is coordinated with the rate of their utilization in metabolism. At low irradiances, these mechanisms serve to optimize light use efficiency, while at high irradiances they operate to dissipate excess excitation energy as heat (Foyer et al. 2012). Porcar-Castell et al. (2008) observed that during the cold days in winter, F_t began to increase immediately after sunrise while F_m' started to decrease about 45 min later. A certain delay between F_m' and F_t was also observed on 18 and 19 September and on 21 September 2012 under HCLN conditions. This phenomenon was explained as consistent with the assumption that the F_t increase corresponds to a reduction of the electron transport chain at sunrise when low temperatures retard the use of ATP and NADPH by the Calvin cycle (Porcar-Castell et al. 2008). As in our study, F_m' and F_t were generally coupled. As observed by Porcar-Castell et al. (2008), 3 general stages could be distinguished in the diurnal variations of F_m' and F_t: firstly, after sunrise F_m' decreased and F_t increased, suggesting increasing heat dissipation together with saturation of the electron transport chain; secondly, during the day both F_m' and F_t changed in a similar manner, indicating the rapid adjustment in non-photochemical quenching to fluctuations in the light environment. C, N and temperature affected the time course of this coupling. Under ambient temperature, it was maintained for 11 of the 12 h light cycle. At increased temperature, the coupling was more variable, i.e. under LCLN, F_m' and F_t were coupled for only 4 of the 12 h light period whereas under HCLN and LCHN, it occurred for 7 h and under HCHN, for 11 h. This provides further evidence for the combined effects of C–N and temperature on fluorescence parameters. Thirdly, before sunset, F_m' increased and F_t increased to a lesser extent; this may be related to a relaxation of non-photochemical energy dissipation and re-oxidation of the electron transport chain. This pattern was also evident in pine leaves (Porcar-Castell et al. 2008), although in *U. rigida* this F_m' increase occurred several hours after sunset (2 to 5 h, depending on treatment).

In the present study, the expression of rETR did not allow an estimation of productivity, since this would require the measurement of absorptance and the proportion of total light absorbed by photosystem II, which depends on bio-optical characteristics of the species and the light history (Johnsen & Sakshaug 2007). Absorptance was determined throughout the day in an experiment with floating thalli (Figueroa et al. 2014) and these data can thus not be used here as the algal thallus in the Moni-PAM was in a fixed position (Fig. 1) and the absorptance would be expected to differ. Absorptance in *Ulva* species is affected by temperature and light conditions (Figueroa et al. 2003, 2009).

During night periods

Maximal values of F_v/F_m were observed at certain times after sunset, depending on C–N and temperature treatments. Under LCLN and HCHN and ambient temperature, maximal values of F_v/F_m were observed about 1 to 1.5 h after sunset, whereas at +4°C, maximal values were observed after 1.5 to 2.5 h. On the other hand, under HCLN no effect of temperature was observed on the time course of F_v/F_m. The earlier maximal F_v/F_m values under increased temperature could be related to faster repair processes and recovery after photoinhibition (Nishiyama et al. 2006).

The negative slope of nighttime decrease in F_v/F_m was affected by the C–N treatments. Slopes were greater under HN than under LN treatments at ambient temperature. However, during the last 2 nights under increased temperature, the negative slope of F_v/F_m decrease was higher in LN treatments and under HCHN than under LCHN. The decrease of photosynthetic yield during the night has previously been attributed to photoinhibitory effects of saturating light pulses (Flexas et al. 2000). To alleviate the side effects of saturating pulses, Porcar-Castell et al.(2008) increased the interval between pulses from 5 to 10 min, but nighttime depression of F_v/F_m was still occasionally observed in cold nights. Thus, Porcar-Castell et al. (2008) recommended decreasing the frequency of saturating pulses during cold nights even further (e.g. every hour), and during daytime, carry out measurements at higher frequencies (e.g. every 5 to 10 min). The latter regime of data collection would still permit long- and short-term adjustments in PSII to be followed. This re-emphasizes the importance of maintaining a constant area of algal thalli under examination to draw accurate conclusions on the true fluorescence levels.

The different time courses of F_m and F_0 at night and F_m' and F_t in the light by the treatments can be interpreted as the effect of C–N and temperature on the redox state and the relaxation of non-photochemical quenching and energy dissipation. The transient high values of F_v/F_m 1 to 3 h after dawn and of $\Delta F/F_m'$ 1 to 3 h after dusk can be an indication of the reported activation by light of the enzyme activities related to CO_2 (Maheshwari et al. 1992) and nitrogen metabolism through oxido-reduction processes mediated by ferredoxin/thioredoxin (Foyer et al. 2012) or by blue-light photoreceptors (Azuara & Aparicio 1985, Rüdiger & López-Figueroa 1992). In vascular plants, changes after dawn and dusk have been related to diurnal patterns of photosynthetic gene expression and are fundamentally controlled by circadian clock regulators with input from non-photosynthetic photoreceptors (Maet al. 2001, Ghassemian et al. 2006). Diurnal variations regulated by non-photosynthetic photoreceptors on pigment accumulation and N metabolism have been reported in *U. rigida* (López-Figueroa & Rüdiger 1991, Figueroa & Viñegla 2001). The decrease of $\Delta F/F_m'$ that we observed was always followed by its increment and recovery at the end of the daily light period for samples at ambient temperature, despite a lower capacity of energy dissipation. This might suggest a reduction of the fraction of the incident energy absorbed, possibly as a consequence of photoprotection of the PSII reaction centers due to a decrease in antenna size (Gordillo et al. 2003). Consistent with this idea, a decrease in chlorophyll *a* was observed under HC, which was higher under a low nitrate supply (see Stengel et al. 2014). Although our data followed the same daily pattern as those obtained using a Diving-PAM with sampling intervals of 3 h (see Stengel et al. 2014), the values of $\Delta F/F_m'$ for identical time periods were always lower in the case of Moni-PAM; it is therefore possible that a decrease in $\Delta F/F_m'$ similar to that described for the night could have taken place during the light period. In our study, the thalli in the Moni-PAM were in a fixed position, receiving a higher dosage of solar radiation than free floating macroalgae moving within tanks, thus presenting canopy conditions. On the other hand, $rETR_{max}$ under outdoor conditions determined by Moni-PAM ranged from 49 to 133 µmol $e^- m^{-2} s^{-1}$ whereas $rETR_{max}$ values obtained in the laboratory by using a PAM 2000 fluorometer, illuminating samples with artificial light from a halogen lamp, were slightly lower (20 to 120 µmol $e^- m^{-2} s^{-1}$). Longstaff et al. (2002) also showed that *in situ* ETR_{max} in *U. lactuca* determined with solar irradiance in a daily cycle was higher than ETR_{max} obtained using artificial light.

Relationship between physical–chemical and physiological variables

The multivariate RDA analysis showed the important role of PAR irradiance. rETR is the positive part in response to high values of PAR whereas high values of $\Delta F/F_m'$, F_m' and (to a lesser extent) F_t are linked to low PAR irradiance. The effect of CO_2 treatment and experimental increase of temperature on the photosynthetic response of algae is low but significant (as recorded through the second axis). The temperature increase of 4°C increased rETR as it has been shown in ETR_{max} in the same experiment by using a PAM 2000 fluorometer (Figueroa et al. 2014). The RDA axes in the nights show that the first axis is associated with the highest values of all the measured photosynthetic variables (F_m, F_0 and F_v/F_m). Interestingly, this axis is strongly associated with the C and N treatments, albeit with opposite effects. Reverse responses of carbon and nitrogen metabolism have been shown in measurements of carbonic anhydrase and nitrate reductase activities during daily cycles in *U. rigida* (Figueroa & Viñegla 2001). Both low C concentrations (mainly when N was high) and higher temperature increased F_m, F_0 and F_v/F_m, while high C concentration (simulation of OA) tended

to reduce them. The 'slow phase' of the fluorescence induction curve represents an induction of Calvin cycle enzyme activity and its subsequent interaction with the electron transport chain (via NADPH) and photochemical and non-photochemical quenching (Krause & Weis 1984). The decline from M to T in the Kautsky fluorescence induction curve is generally recognized as a reflection of activation of the Calvin-Benson cycle enzymes (Govindjee 1995). The resulting increase in CO_2 fixation rate and NADPH re-oxidation has a flow-through effect back up the photosynthetic electron transport chain, yielding a higher photochemical quenching (Renger & Schreiber 1986). The decrease of F_v/F_m during the night could also be related to chlororespiration. Chlororespiration, in contrast to photorespiration, only occurs in the dark, and at very low irradiances when the photosynthetic machinery is not operative (Peltier & Cournac 2002). It has been proposed as a mechanism to maintain ATP syntheses in the active state in the dark, acting as a sink of photosynthetically generated reducing equivalent NAD(P)H (Beardall et al. 2003).

In conclusion, our data suggest that OA (i.e. our HC treatment) under the low nitrate conditions of the Mediterranean (LN treatment) could produce a decrease in the photosynthetic yield of *U. rigida*, whereas an increase in temperature could slow the decrease of $\Delta F/F_m'$ in the afternoon. Thus, the negative effects of OA and oligotrophication expected in the area within this century (Mercado et al. 2012) could be mitigated by the expected increase in temperature. Data with high temporal resolution such as that provided by the Moni-PAM data are scarce for plants, and this is the first study presenting data for a macroalga. As demonstrated here, such measurements are particularly useful when attempting to obtain accurate time-integrated data, such as integrated rETR or the relation of rETR versus irradiance during a complete daily cycle. Furthermore, continuous recordings of fluorescence parameters (including nighttime) have revealed important information regarding transient physiological processes in PSII that are difficult to observe. Additionally, observations of nighttime processes are rare for vascular plants and to our knowledge so far not previously reported for seaweeds; our results show that important dynamics occur that vary according to environmental conditions.

Acknowledgements. We gratefully acknowledge the financial contributions for the GAP 9 workshop 'Influence of the pulsed-supply of nitrogen on primary productivity in phytoplankton and marine macrophytes: an experimental approach' at the University of Malaga, sponsored by Walz GmbH facilitating the use of several PAM fluorometers, by the Redox company, the University of Malaga, the Ministry of Economy and Competitivity of the Spanish Government (Acción Complementaria CTM2011-15659-E), the Project Interacid (RNM5750) of the Junta de Andalucía and the Spanish Institute of Oceanography. P.S.M.C.-P. gratefully acknowledges financial support through a grant to conduct the PhD ('Becas-Chile', CONICYT by the Ministry of Education of the Republic of Chile.

LITERATURE CITED

Axelsson L, Ryberg H, Beer S (1995) Two modes of bicarbonate utilization in the marine green macroalga *Ulva lactuca.* Plant Cell Environ 18:439–445

Azuara MP, Aparicio PJ (1985) Spectral dependence of photoregulation of inorganic nitrogen metabolism in *Chlamydomonas reinhardii.* Plant Physiol 77:95–98

Barták M, Vácziu P, Hákjek J (2012) Photosynthetic activity in three vascular species of Spitbergen vegetation during summer season in response to microclimate. Pol Polar Res 33:443–462

Beardall J, Quigg A, Raven JA (2003) Oxygen consumption: photorespiration and chlorespiration. In: Larkum AW, Douglas SE, Raven JA (eds) Photosynthesis in algae. Kluwer Academic Publishers, Dordrecht, p 157–181

Beer S, Larsson C, Poryan O, Axelsson L (2000) Photosynthetic rates of *Ulva* (Chlorophyta) measured by pulse amplitude modulated (PAM) fluorometer. Eur J Phycol 35:69–74

Brewer PG (1997) Ocean chemistry of the fossil fuel CO_2 signal: the haline signal of 'business as usual'. Geophys Res Lett 24:1367–1369

Cabello-Pasini A, Figueroa FL (2005) Effect of nitrate concentration on the relation between photosynthetic oxygen evolution and electron transport rate in *Ulva rigida* (Chlorophyta). J Phycol 41:1169–1177

Caldeira K, Wickett ME (2003) Anthropogenic carbon and ocean pH. Nature 425:365

Doney SC, Fabry VJ, Feely RA, Kleypas JA (2009) Ocean acidification: the other CO_2 problem. Annu Rev Mar Sci 1:169–192

Enríquez S, Borowitzka MA (2011) The use of the fluorescence signal in studies of seagrasses and macroalgae. In: Suggett DJ, Borowitzka M, Ondrej P (eds) Chlorophyll *a* fluorescence in aquatic sciences: methods and applications. Developments in applied phycology, Vol 4. Springer Science+Business Media, Dordrecht, p 187–208

Figueroa FL, Viñegla B (2001) Effects of solar UV radiation on photosynthesis and enzyme activities (carbonic anhydrase and nitrate reductase) in marine macroalgae from southern Spain. Rev Chil Hist Nat 74:237–249

Figueroa FL, Salles S, Aguilera J, Jiménez C and others (1997) Effects of solar radiation on photoinhibition and pigmentation in the red alga *Porphyra leucosticta.* Mar Ecol Prog Ser 151:81–90

Figueroa FL, Conde-Álvarez R, Gómez I (2003) Relations between electron transport rates determined by pulse amplitude modulated chlorophyll fluorescence and oxygen evolution in macroalgae under different light conditions. Photosynth Res 75:259–275

Figueroa FL, Martínez B, Israel A, Neori A and others (2009) Acclimation of Red Sea macroalgae to solar radiation: photosynthesis and thallus absorptance. Aquat Biol 7: 159–172

Figueroa FL, Jerez C, Korbee N (2013) Use of *in vivo* chlorophyll fluorescence to estimate photosynthetic activity and biomass productivity in microalgae grown in different culture systems. Lat Am J Aquatic Res 41:801–819

Figueroa FL, Bonomi Barufi J, Malta EJ, Conde-Álvarez R and others (2014) Short-term effects of increasing CO_2 , nitrate and temperature on three Mediterranean macroalgae: biochemical composition. Aquat Biol 22:177–193

Flexas J, Briantais JM, Cerovic Z, Medrano H, Moya I (2000) Steady-state and maximum chlorophyll fluorescence responses to water stress in grapevine leaves: a new remote sensing system. Remote Sens Environ 73:283–297

Foyer CH, Neukermans J, Quavel G, Noctor G, Harbinson J (2012) Photosynthetic control of electron transport and the regulation of gene expression. J Exp Bot 63: 1637–1661

Gao K, Aruga Y, Asada K, Ishihara T, Akano T, Kiyohara M (1993) Calcification in the articulated coralline alga *Corallina pilulifera* with special reference to the effect of elevated CO_2 concentration. Mar Biol 117:129–132

Ghassemian M, Lutes J, Tepperman JM, Chang HS and others (2006) Integrative analysis of transcript and metabolite profiling data sets to evaluate the regulation of biochemical pathways during photomorphogenesis. Arch Biochem Biophys 448:45–59

Giordano M, Beardall J, Raven JA (2005) CO_2 concentrating mechanisms in algae: mechanisms, environmental modulation, and evolution. Annu Rev Plant Biol 56: 99–131

Gordillo FJL, Niell FX, Figueroa FL (2001) Non-photosynthetic enhancement of growth by high CO_2 level in the nitrophilic seaweed *Ulva rigida* C. Agardh (Chlorophyta). Planta 213:64–70

Gordillo FJL, Figueroa FL, Niell FX (2003) Photon and carbon use efficiency in *Ulva rigida* at different CO_2 and N levels. Planta 218:315–322

Govindjee (1995) Sixty-three years since Kautsky: chlorophyll *a* fluorescence. Aust J Plant Physiol 22:131–160

Harley CDG, Anderson KM, Demes KW, Jorve JP, Kordas RL, Coyle TA, Graham MH (2012) Effects of climate change on global seaweed communities. J Phycol 48: 1064–1078

Henley WJ, Levavasseur G, Franklin LA, Lindley ST, Ramus J, Osmond CB (1991) Diurnal responses of photosynthesis and fluorescence in *Ulva rotundata* acclimated to sun and shade in outdoor culture. Mar Ecol Prog Ser 75: 19–28

Hepburn CD, Pritchard DW, Cornwall CE, McLeod RJ, Beardall J, Raven JA, Hurd CL (2011) Diversity of carbon use strategies in a kelp forest community: implications for a high CO_2 ocean. Glob Change Biol 17:2488–2497

Huovinen P, Matos J, Sousa-Pinto I, Figueroa FL (2006) The role of ammonium in photoprotection against high irradiance in the red alga *Grateloupia lanceola.* Aquat Bot 84: 308–316

Hurd C, Hepburn C, Currie K, Raven J, Hunter A (2009) Testing the effects of ocean acidification on algal metabolism: considerations for experimental designs. J Phycol 45:1236–1251

Ihnken S, Eggert A, Beardall J (2010) Exposure times in rapid light curves affect photosynthetic parameters in algae. Aquat Bot 93:185–194

Johnsen G, Sakshaug E (2007) Biooptical characteristics of PSII and PSI in 33 species (13 pigment groups) of marine phytoplankton, and the relevance for pulse-amplitude-modulated and fast-repetition-rate fluorometry. J Phycol 43:1236–1251

Korbee N, Figueroa FL, Aguilera J (2005) Effect of light quality on the accumulation of photosynthetic pigments, proteins and mycosporine-like amino acids in the red alga *Porphyra leucosticta* (Bangiales, Rhodophyta). J Photochem Photobiol B 80:71–78

Krause GH, Weis E (1984) Chlorophyll fluorescence as a tool in plant physiology. II. Interpretation of fluorescence signals. Photosynth Res 5:139–157

Leps J, Smilauer P (2003) Multivariate analysis of ecological data using CANOCO. Cambridge University Press, New York, NY

Longstaff BJ, Kildea T, Runcie JW, Cheshire A and others (2002) An *in situ* study of photosynthetic oxygen evolution exchange and electro transport rate in the marine macroalga *Ulva lactuca* (Chlorophyta). Photosynth Res 74:281–293

López-Figueroa F, Rüdiger W (1991) Stimulation of nitrate net uptake and reduction by red and blue light and the reversion by far-red light in the green alga *Ulva rigida.* J Phycol 27:389–394

Ma L, Li J, Qu L, Hager J, Chen Z, Zhao H, Deng XW (2001) Light control of Arabidopsis development entails coordinated regulation of genome expression and cellular pathways. Plant Cell 13:2589–2607

Maheshwari V, Dwivedi U, Bhardwaj R, Mishra M (1992) Mechanism of reductive photoactivation of enzyme of C_4 pathway. J Biosci 17:183–192

Marek MV, Kalina J, Matouskova M (1995) Response of photosynthetic carbon assimilation of Norway Spruce exposed to long-term elevation of CO_2 concentration. Photosynthetica 31:209–220

Martin S, Gattuso JP (2009) Response of Mediterranean coralline algae to ocean acidification and elevated temperature. Glob Change Biol 15:2089–2100

Martínez B, Arenas F, Rubal M, Burgués S and others (2012) Physical factors driving intertidal macroalgae distribution: physiological stress of a dominant fucoid at its southern limit. Oecologia 170:341–353

McMinn A, Ryan K, Gademann R (2003) Diurnal changes of Antarctic fast ice algal communities determined by pulse amplitude modulation fluorometry. Mar Biol 143: 359–367

Meehl GA, Stocker TF, Collins WD, Friedlingstein P and others (2007) Global climate projections. In: Solomon S, Qin D, Manning M, Chen Z and others (eds) Climate change 2007: the physical science basis. Contribution of Working Group I to the Fourth Assessment Report of the Intergovernmental Panel on Climate Change. Cambridge University Press, Cambridge, p 749–845

Mercado JM (2008) Effects of the acidification on photosynthesis and growth of marine algae: a reappraisal of the laboratory data and their applicability to the natural habitats. In: Hagen KN (ed) Algae: nutrition, pollution control and energy sources. Nova Science Publishers, New York, NY, p 1–20

Mercado JM, Cortés D, Ramírez T, Gómez F (2012) Decadal weakening of the wind-induced upwelling reduces the impact of nutrient pollution in the Bay of Málaga (western Mediterranean Sea). Hydrobiologia 680:91–107

Mercado JM, Gordillo FJL, Figueroa FL, Niell FX (1998) External carbonic anhydrase and affinity for inorganic carbon in intertidal macroalgae. J Exp Mar Biol Ecol 221: 209–220

Nishihara GN, Terada R, Noro T (2005) Effect of temperature and irradiance on the uptake of ammonium and nitrate by *Laurencia brongniartii* (Rhodophya, Ceramiales). J Appl Phycol 17:371–377

Nishiyama Y, Allarkhverdiev SI, Murata N (2006) A new paradigm for the action of reactive oxygen species in the photoinhibition of photosystem II. Biochim Biophys Acta 1757:742–749

Nitschke U, Connan S, Stengel D (2012) Chlorophyll *a* fluorescence responses of temperate Phaeophyceae under submersion and emersion regimes: a comparison of a rapid and steady-state light curves. Photosynth Res 114: 29–42

Olischläger M, Bartsch I, Gutow L, Wiencke C (2013) Effects of ocean acidification on growth and physiology of *Ulva lactuca* (Chlorophyla) in a rockpool-scenario. Phycol Res 61:180–190

Orr JC, Fabry VF, Aumont O, Bopp L and others (2005) Anthropogenic ocean acidification over the twenty-first century and its impact on calcifying organisms. Nature 437:681–686

Pastenes C, Horton P (1996) Effect of high temperature on photosynthesis in beans. II. CO_2 assimilation and metabolite contents. Plant Physiol 112:1253–1260

Pelejero C, Calvo E, Hoegh-Guldberg O (2011) Paleoperspectives on ocean acidification. Trends Ecol Evol 25: 332–344

Peltier G, Cournac L (2002) Chlororespiration. Annu Rev Plant Biol 53:523–550

Pérez-Lloréns JL, Vergara J, Pino R, Hernández I, Peralta G, Niell FX (1996) The effect of photoacclimation on the photosynthetic physiology of *Ulva curvata* and *Ulva rotundata* (Ulvales, Chlorophyta). Eur J Phycol 31:349–359

Porcar-Castell A, Pfündel E, Korhonen E, Juurola E (2008) A new monitoring PAM fluorometer (*MONI-PAM*) to study the short- and long-term acclimation of photosystem II in field conditions. Photosynth Res 96:173–179

Raggio J, Pintado A, Vivas M, Sancho LG and others (2014) Continuous chlorophyll fluorescence, gas exchange and microclimate monitoring in a natural soil crust habitat in Tabernas badlands, Almería, Spain: progressing towards a model to understand productivity. Biodivers Conserv 23:1809–1826

Ralph PJ, Gademann R (2005) Rapid light curves: a powerful tool to asses photosynthetic activity. Aquat Bot 82: 222–237

Ramírez T, Cortés D, Mercado JM, Vargas-Yáñez M, Sebastián M, Liger E (2005) Seasonal dynamics of inorganic nutrients and phytoplankton biomass in the NW Alboran Sea. Estuar Coast Shelf Sci 65:654–670

Raven JA (2011) Effects on marine algae of changed seawater chemistry with increasing atmospheric CO_2. Biol Environ Proc R Ir Acad B 111:1–17

Raven JA, Cockell CS, La Rocha CL (2008) The evolution of inorganic carbon concentrating mechanisms in photosynthesis. Philos Trans R Soc Lond B Biol Sci 363: 2641–2650

Renger G, Schreiber U (1986) Practical applications of fluorometric methods to algae and higher plant research. In: Govindjee, Amesz J, Fork DC (eds) Light emission by plants and bacteria. Academic Press, Orlando, FL, p 589–619

Riebesell U, Schulz KG, Bellerby RGJ, Botros B and others (2007) Enhanced biological carbon consumption in a high CO_2 ocean. Nature 450:545–548

Ritchie RJ (2008) Fitting light saturation curves measured using modulated fluorometry. Photosynth Res 96:201–215

Roleda MY, Hurd CL (2012) Seaweed responses to ocean acidification. In: Wiencke C, Bischof K (eds) Seaweed biology. Springer, Berlin, p 407–431

Rüdiger W, López-Figueroa F (1992) Photoreceptors in algae. Annu Rev Photochem Photobiol 55:949–954

Runcie JW, Paulo D, Santos R, Sharon Y, Beer S, Silva J (2009) Photosynthetic responses of *Halophila stipulacea* to a light gradient. I. *In situ* energy partitioning of non-photochemical quenching. Aquat Biol 7:143–152

Russell BD, Connell SD (2012) Origins and consequences of global and local stressors: incorporating climatic and non-climatic phenomena that buffer or accelerate ecological change. Mar Biol 159:2633–2639

Schreiber U, Bilger W (1993) Progress in chlorophyll fluorescence research: major developments during the past year in retrospect. In: Lüttge H, Ziegler HE (eds) Progress in botany, Vol 54. Springer, Berlin, p 151–173

Stengel DB, Conde-Álvarez R, Connan S, Nitschke U and others (2014) Short-term effects of CO_2, nutrients and temperature on three marine macroalgae under solar radiation. Aquat Biol 22:159–176

Underwood T (1997) Experiments in ecology: their logical design and interpretation using analysis of variance. Cambridge University Press, Cambridge

Vergara JJ, Bird KT, Niell FX (1995) Nitrogen assimilation following NH_4^+ pulses in the red alga *Gracilariopsis lemaneiformis*: effect on C metabolism. Mar Ecol Prog Ser 122:253–263

Webb WL, Newton M, Starr D (1974) Carbon dioxide exchange of *Alnus rubra*: a mathematical model. Oecologia 17:281–291

Zar JH (2009) Biostatistical analysis. Prentice Hall, Princeton, NJ

Submitted: December 9, 2013; Accepted: July 18, 2014

Proofs received from author(s): October 6, 2014